Reduction of the Gibbs Phenomenon Applied on Nonharmonic Time Base Distortions

Fjo De Ridder, Rik Pintelon, *Fellow, IEEE*, Johan Schoukens, *Fellow, IEEE*, and Anouk Verheyden

***Abstract*—A sine wave fitting procedure for characterizing measurements of a periodic signal in the presence of additive noise and an unknown time base distortion is presented. If the time base distortion is modeled by a Fourier series, it suffers from the Gibbs phenomenon (ringing) at the borders of the data record. Usually, this is solved by ignoring data samples at the borders. The latter is unacceptable for very short data records where measuring a sample is (very) expensive and/or (very) time consuming. This paper presents a solution that suppresses the ringing in the estimated time base distortion without ignoring data samples at the borders. The theory is illustrated on simulations and on real vessel density in the wood of a mangrove tree from Kenya *(Rhizophora mucronata)*.**

***Index Terms*—Accretion rate, dendrochronology, Gibbs phenomenon, mangrove, ringing, time base distortion.**

I. Introduction and Outline of the Problem

THE estimation of a harmonic signal in the presence of additive noise and an unknown time base distortion (TBD) has been studied intensively in the literature [1]–[5]. Two different approaches can be distinguished. The first starts from a single observation (data record) of the harmonic signal and uses a parametric time base distortion model [1], [2], [5]. The second uses several well-chosen observations of the harmonic signal and a nonparametric time base distortion representation [3], [4]. In general, the first approach suffers from ringing at the borders of the data record, which is not the case for the second approach. In [2], the problem is solved by deleting samples at the borders. This paper studies the estimation of a harmonic signal in the presence of additive noise and a time base distortion, starting from a (very) short data record, where measuring one sample is (very) expensive and/or (very) time consuming.

Such measurements can, for example, be encountered in tropical dendrochronology. Tropical tree species often lack annual growth rings (see [6]). Furthermore, even in tree species that display growth rings, ring width data, a measure for the productivity of the tree, may not always provide environmental information [7]–[9]. However, detailed anatomical measurements of wood have the potential to give information about the past environment in which the tree grew. For instance, changes in vessel density and diameters (vessels are tube-like cells responsible for the water transport from the roots to the leaves of a plant) may reflect changes in environmental conditions (e.g., [9]–[11]). Detecting these changes is of major importance to understand forest dynamics and to ensure a sustainable management of the forests.

In the study described in this paper, the vessel density in a mangrove tree was measured manually by counting the vessels employing a microscope, aided with image analysis software (Analysis 3.0). Counting the density along a radial axis from bark to pith takes about a full day of manual work (depending on the size of the tree) [9]. Besides the cost and time, the data record can be fairly short, therefore ignoring data in order to reduce ringing is clearly not satisfactory. Other data records suffering from the same problems, e.g., time base distortions due to changes in growth or accretion rate, include sclerosponges [12], [14], speleothems [13], [15], corals [16]–[20], bivalves [21], [22], sediments [23]–[25], and ice cores [26].

This paper proposes a sine wave fitting procedure that suppresses ringing of the estimated parametric time base distortion model without data removal at the borders.

II. Sampling and Methodology

A stem disc of the mangrove *R. mucronata* was collected in November 1999 from Gazi Bay, Kenya (39.5°E, 4.4°S), located 40 km south of Mombasa. The sample is now part of the xylarium of the Royal Museum for Central Africa (RMCA), Tervuren, Belgium (Tervuren wood collection, accession number Tw55891).

The rainfall along the Kenyan coast shows a bimodal distribution, which is locally expressed in terms of the long rains (from April to July) and the short rains (from October to November), with a mean annual precipitation of 1144 mm (1890–1985) [27]. The temperature ranges from 23.3 to 29.9 °C with a mean annual temperature of 26.4 °C (1931–1990) [27].

The stem disc (Fig. 1) was air dried and its transversal section sanded (grain 100 to 1200). Prior to measurements, the sample was treated with white wasco-crayons, in order to enhance the delimitation of vessel elements. The vessel density was measured directly on the polished stem disc, along a radial transect from bark to pith in adjacent windows (Fig. 2). Window size was set to 300 μm height and 2100 μm width. The number of vessels in each area was counted at an optical magnification of 12× using image analysis software (AnalySIS 3.0) and recalculated to the number of vessels per square millimeter.

Manuscript received August 2, 2004; revised February 9, 2005. This work was supported by the Fund for Scientific Research (FWO-Vlaanderen), the Flemish Government (GOA-IMMI), and the Belgian Program on Interuniversity Poles of Attraction under the Belgian Prime Minister's Office, Science Policy Programming (IUAP 5).

F. De Ridder, R. Pintelon, and J. Schoukens are with the Department of Electricity and Instrumentation, Team B: System Identification, Vrije Universiteit Brussel, B-1050 Brussels, Belgium (e-mail: federid@pop.vub.ac.be).

A. Verheyden is with the Laboratory of General Botany and Nature Management, Vrije Universiteit Brussel, B-1050 Brussels, Belgium.

Digital Object Identifier 10.1109/TIM.2005.847201

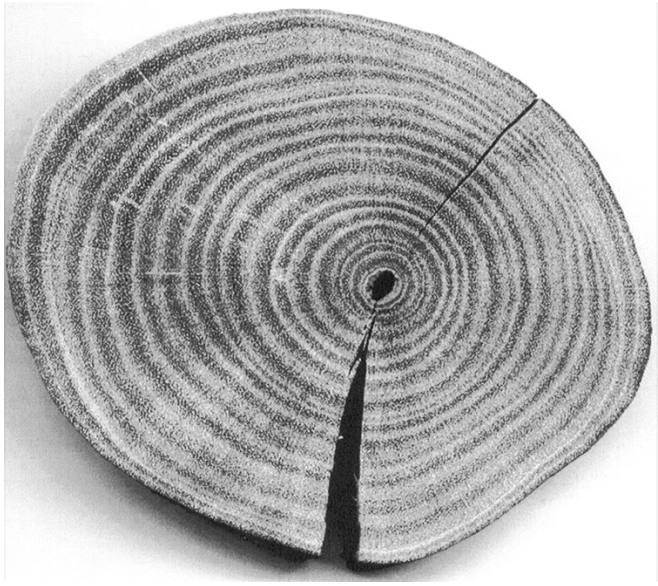

Fig. 1. Cross-section of a mangrove tree. The dark rings correspond to low vessel density and the light rings correspond to high densities [36].

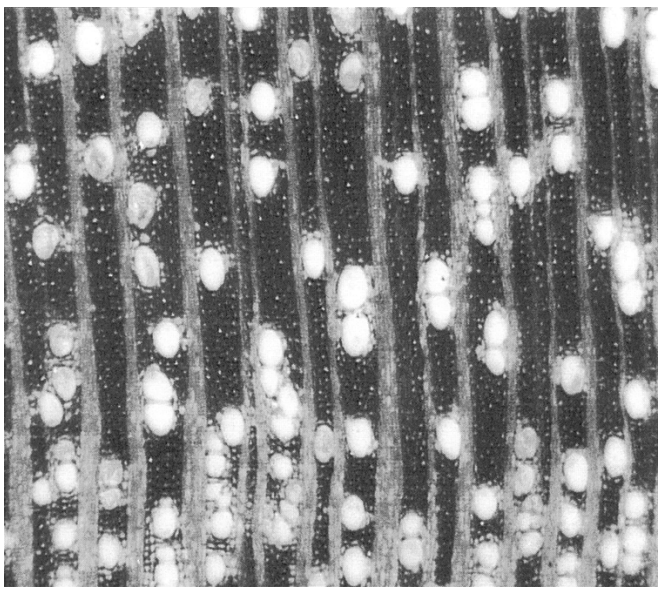

Fig. 2. Microscopic view of stem cross-section illustrating the vessels (white ovals).

III. Model

A sine wave fitting procedure [28] is combined with the TBD identification technique of [1] in order to identify the harmonic content of the data. The signal model must describe the physical signal as closely as possible. This reduces the modeling errors and therefore increases the precision of the results. It is assumed that the continuous-time signal model $s(t)$ for the measurements is given by

$$s(t) = \sum_{k=1}^{h} [A_k \cos(k\omega t) + A_{k+h} \sin(k\omega t)] \tag{1}$$

where t is the time variable, A_k and A_{k+h} are the unknown amplitudes of the kth harmonic ($k \in \{1, \ldots, h\}$), and ω is the unknown fundamental angular frequency. The analog signal $s(t)$ is sampled at the time instances

$$t_n = [n + g(n)]T_s \tag{2}$$

where $n \in \{0, \ldots, N-1\}$, with N the number of samples, $T_s = 1/f_s$ the sample period, f_s the sampling frequency, and $g(n)$ the deterministic, unknown TBD. The time instance t_n is the time the specimen took to grow the sampling distance. Variations in growth rate will consequently cause variations in the sample moments, described by the value of the TBD $g(n)$. In order to characterize this TBD, parametric models are used. In general the TBD can be expanded in any set of (orthogonal) basis functions $\phi_l(n)$

$$g(n) = \sum_{l=1}^{b} B_l \phi_l(n) \tag{3}$$

where B_l are the unknown coefficients of the TBD ($l \in \{1, \ldots, b\}$). A good choice of basis functions will limit the number of coefficients needed to describe the TBD. Two orthogonal bases are discussed in this paper: the basis of the orthonormal Legendre polynomials and the basis of trigonometric functions.

If the time base distortion is reconstructed for a record where an exponentially decreasing accretion rate (without much variation) is assumed, a polynomial model would probably perform better. On the other hand, if the accretion rate is influenced by climatological conditions, which vary mainly with a yearly periodicity, a Fourier basis would probably perform better. Considering that we do not know in advance which effect will overrule the other, both the polynomial and Fourier basis set are used. Hiatuses (stops in growth) are unlikely to occur in mangrove trees [9], but no additional constraints such as smoothness, continuity, etc., have been implemented in order to keep the number of applications as wide as possible. On other occasions, when accretion hiatuses are present (e.g., [29]), B-splines or other sets can be more useful than the basis sets used in this paper.

A. Othonormal Legendre Polynomials

The orthonormal Legendre polynomials [30] have been chosen in order to avoid numerical problems in the estimation of the parameters. Note that the offset and the linear term are not used. The reason for this is that the corresponding coefficients cannot be identified uniquely: i) the offset in the TBD can be rewritten as a linear phase shift (time delay) in the signal model and ii) the coefficient of the linear term acts as a shift of the fundamental frequency. To show this, suppose an offset α and a linear trend $\beta n T_s$ in the TBD $g(n) = \alpha + \beta n T_s + h(n)$, with $h(n)$ the remaining part of the TBD. The argument in (1) can be rewritten so that the offset and linear trend are replaced by a change in the angular frequency and a linear phase shift

$$\begin{aligned} k\omega\left[nT_s + g(n)T_s\right] &= k\omega\left[nT_s + \alpha T_s + \beta n T_s + h(n)T_s\right] \\ &= k\omega[1+\beta]\left[nT_s + \frac{h(n)}{1+\beta}T_s\right] + k\omega(\alpha T_s) \\ &= k\omega_1\left[nT_s + h_1(n)T_s\right] + \phi(\omega) \end{aligned} \tag{4}$$

where ω_1 is the shifted angular frequency, ϕ the phase shift, and $h_1(n)$ the remaining TBD.

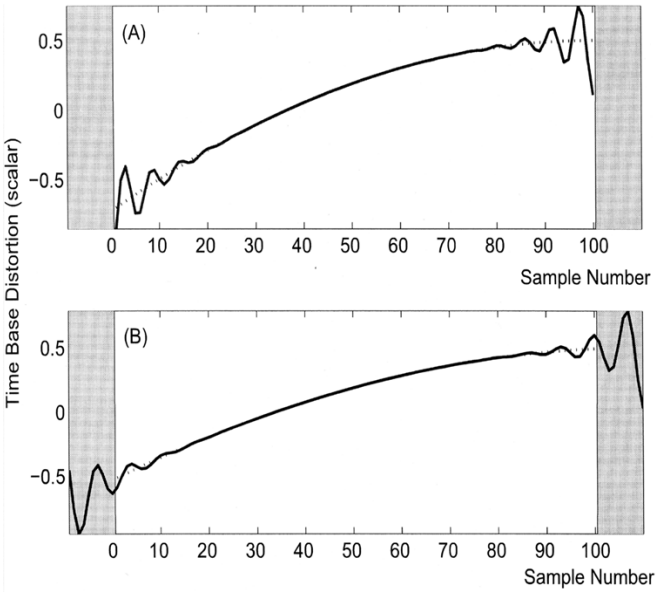

Fig. 3. Conceptual illustration of the Gibbs phenomenon (ringing). Measurement window (white rectangle), enlarged borders (gray rectangles), modeled TBD (full line), and unknown TBD (dotted line).

B. Trigonometric Series and the Gibbs Phenomenon

The parametric representation of the TBD as a Fourier series is given by

$$g(n) = \sum_{l=1}^{b/2} \left[B_l \cos(2\pi n l T_s) + B_{l+b/2} \sin(2\pi n l T_s) \right]. \quad (5)$$

In the examples used in this paper, no prior knowledge of the shape of the TBD is available, so the polynomial model may intuitively be a more obvious choice to describe the unknown TBD. Moreover, there is no reason why the TBD model should be periodic. So, ringing will occur when (5) is used to approximate a nonperiodic TBD.

In [2], it is proposed to use only a part of the complete measurement period: some points near the borders are ignored during the fit. This reduces ringing considerably. As was pointed out, each measurement point is of high value, so dropping measurements is not ideal. For that reason an alternative is designed to reduce ringing in the TBD model: extra samples are added at the borders. These extra samples will be ignored in the final estimation of the model parameters but allow the procedure to reduce ringing inside the measurement window. Fig. 3(a) shows a TBD model, which is estimated in the initial measurement window. Notice the Gibbs phenomenon, which mainly acts near the borders. Fig. 3(b) shows the same TBD, but this time some extra space is created outside the measurement window. Because ringing occurs mainly at the borders, it is exported mostly outside the measurement window. After the model is matched, these extra borders and most of ringing are dropped.

IV. Estimation of the Model Parameters A_k, B_l, and ω

A. Definition of the Estimators

The parameters of the signal model and of the TBD model are estimated simultaneously by minimizing a cost function with respect to an extended parameter vector

$$\theta = [\omega, A_0, \ldots, A_h, B_1, \ldots, B_b]^T \quad (6)$$

including not only the signal parameters but also the TBD model parameters. The optimal set of parameters in the least square sense is given by

$$\hat{\theta} = \arg\min_{\theta} K_{\mathrm{nls}}(\theta). \quad (7)$$

The explicit expression of the cost function is

$$K_{\mathrm{nls}} = \frac{1}{2} \sum_{n=1}^{\tilde{N}} \left[s(n) - \left(A_0 + \sum_{k=1}^{h} \left[A_k \sin(k\tilde{\omega} t_n) + A_{k+h} \cos(k\tilde{\omega} t_n) \right] \right) \right]^2 \quad (8)$$

where $s(n)$ is the nth sample, t_n is defined in (2) and (3), and A_k and A_{k+h} are defined in (1). For the minimization of (8) a Levenberg–Marquardt algorithm is preferred in order to improve the convergence. Further, each row in the Jacobian was scaled in order to improve the numerical conditioning. When the polynomial or trigonometric model of the TBD with unchanged borders is used, $\tilde{N} = N$, with N the number of samples, and $\tilde{\omega} = \omega$, with ω defined in (1); when samples are dropped near each border $\tilde{N} = N_s$, with $N_s = N - 2q$ the remaining number of samples, and $\tilde{\omega} = \omega$; when the borders are enlarged with q samples at each border, $\tilde{N} = N$ and $\tilde{\omega} = \omega \cdot N_L/N$, with $N_L = N + 2q$. We will refer to the model where samples are dropped as the *reduced model* and to the model with enlarged borders as the *enlarged model*. Notice that if the fundamental frequency in the reduced model were rescaled, as is done in the enlarged model, ringing would appear again.

B. Starting Point Problem

The identification consists of a sequence of four steps which are only summarized in this paper. First, we will discuss how the set of parameters is estimated when the measurement window is not altered (model with $\tilde{N} = N$ and $\tilde{\omega} = \omega$), i.e., we will focus on the polynomial and the trigonometric model of the TBD, where the borders are not altered. The estimation of the initial values is done in precisely the same way as in [2].

1) A nonparametric estimation of the TBD is performed: a TBD acts as a phase modulation, characterized in the spectrum by the lines appearing around the harmonics. The TBD can be isolated by employing a frequency window around the first harmonic in order to cut out an estimate of its spectrum, $\hat{G}$. The calculation of the estimate can be done by shifting the spectrum to dc and then by calculating the inverse Fourier transform.

2) The initial values of the coefficients are generated by matching the proposed model to this nonparametric estimate of the TBD.
3) Also, the sampling moments are calculated using (3).
4) An initial estimation of the amplitudes A_k and fundamental frequency ω of the signal is done by minimizing a least squares cost function, in the same way as in [6], but on the newly calculated sampling moments. Mostly, an initial estimation of the fundamental frequency can be done visually by counting the number of peaks in the signal.

For the reduced model, with $\tilde{N} = N_s$ and $\tilde{\omega} = \omega$, the estimation of initial values remains unchanged. In order to gather starting values for the enlarged model, with $\tilde{N} = N$ and $\tilde{\omega} = \omega \cdot N_L/N$, a larger measurement window is created, consisting of the original one, neighbored at the left by the q last observations and at the right by the q first observations. The procedure will still induce ringing and will thus not estimate the parameters correctly. Regardless, the initial values seem to be sufficient to converge toward a good set of parameters that minimize the cost function (7). For both the reduced and enlarged model, steps 2) to 4) remain unaffected.

C. Advantages and Disadvantages of the Different Approaches

The main advantage of the polynomial model is that no ringing occurs, but the numerical conditioning is worse than for the other trigonometric base based models. Therefore, when a detailed description of the TBD is desired and a lot of basis functions are used, the trigonometric models may be preferred. An extra feature of the trigonometric models is that they can absorb an inaccurate estimation of the initial angular frequency, because this would cause a linear trend in the TBD model. The polynomial model cannot absorb this, because the linear coefficient is not estimated. The linear coefficient β as defined in (4) can be removed by changing the fundamental angular frequency ω to ω_1

$$\omega_1 = \omega(1 + \beta). \tag{9}$$

V. Results of Study Based on Simulation

A. Comparison of the Different Models

In this section a harmonic signal, distorted by a nonperiodic TBD, is simulated. No additive noise was added in order to concentrate on the systematic errors caused by ringing. First, the polynomial model for the TBD is used. Next the trigonometric model is employed, without arrangements to reduce ringing. Finally the reduced and enlarged model are used. These different estimates for the TBD are compared, employing the residual cost function as criterion. The harmonic signal is constructed by a sinus with frequency 8 Hz on a grid of 100 samples ($[1, \ldots, N]/N$, with $N = 100$). Because certain biota have an exponentially decreasing growth rate [31], [32], an exponential decreasing TBD was chosen in the simulation. The offset and the linear trend were removed from the TBD

One harmonic is used to reconstruct the signal, while the number of parameters used in the TBD model was 14, regardless of the model (trigonometric or polynomial). Fig. 4 shows

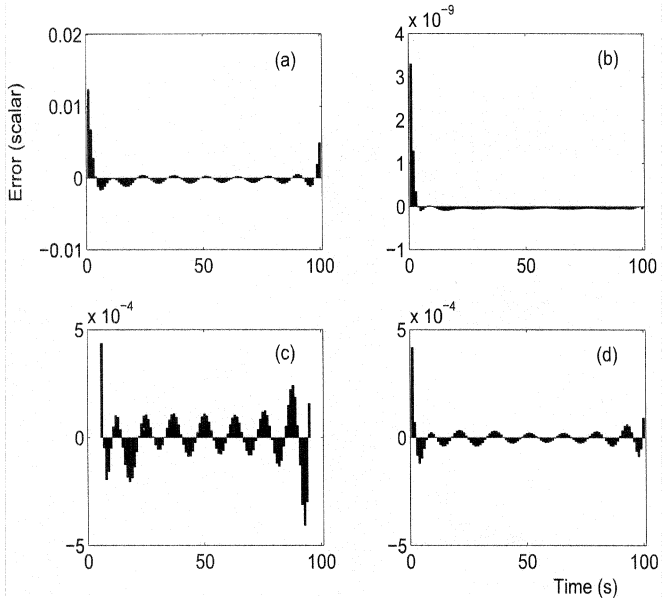

Fig. 4. The absolute error between the estimated TBD and the TBD used in the simulation for (a) the Fourier model, (b) the polynomial model, (c) the reduced Fourier model, and (d) the enlarged Fourier model.

the difference between the estimated and true TBD as well as the original one. Comparison revealed the following.

1) The polynomial model (order 16, 14 coefficients) was able to reconstruct the TBD with hardly any error. A residual cost function of 4×10^{-16} was found.
2) The Fourier model, without any arrangements against the leakage converged toward a residual cost function of 1.2×10^{-2}.
3) The reduced Fourier model, where 10% of the measurements were not used to match the model, had a residual cost function of 4×10^{-4}. This value is already corrected for the reduction of samples: because now only 90 samples were used to match the model, the cost function is evidently lower [34]

$$K_{\text{corr}} = K_{\text{nls}} \frac{N - n_\theta}{N_s - n_\theta} \tag{10}$$

where K_{nls} is the residual cost function, N the total number of samples (here: 100), N_s the number of samples on which the model is matched (here 90), and n_θ the number of model parameters (here 14+2+1). We can conclude that the ringing contribution to the residual cost function is reduced by a factor of 30, but at the cost of removing ten samples and hence lack of knowledge of the TBD at these points.
4) When each border was enlarged with 10% of the total sample number (enlarged model), a residual cost function of 2.8×10^{-5} is found, which is 14 times smaller than in (3) and more than 400 times smaller than (2). The benefit is that no samples were lost at the borders, but because the total sample window is enlarged, the frequency resolution increases, while the number of TBD parameters b remains equal. Consequently, the bandwidth of the TBD model becomes smaller (only the first lines were used).

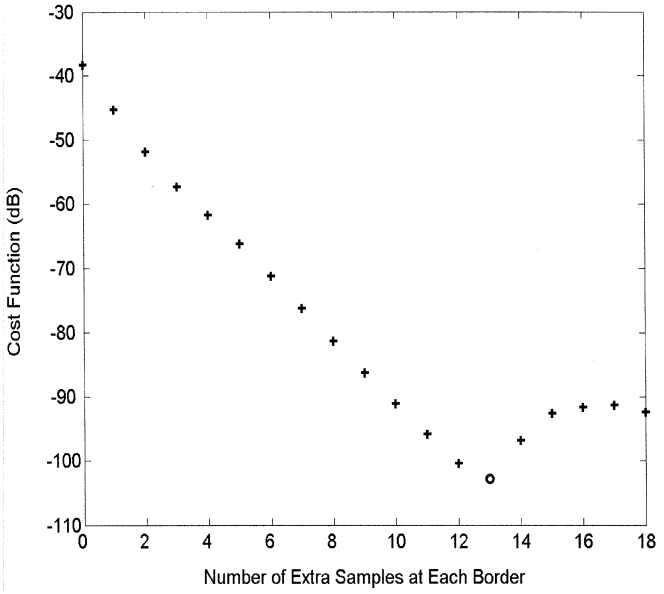

Fig. 5. The cost function as function of the number of extra samples at the border. An optimum ("o") is reached when the decrease, caused by reducing the ringing, is compensated by an increase of the cost function, caused by the decreasing bandwidth.

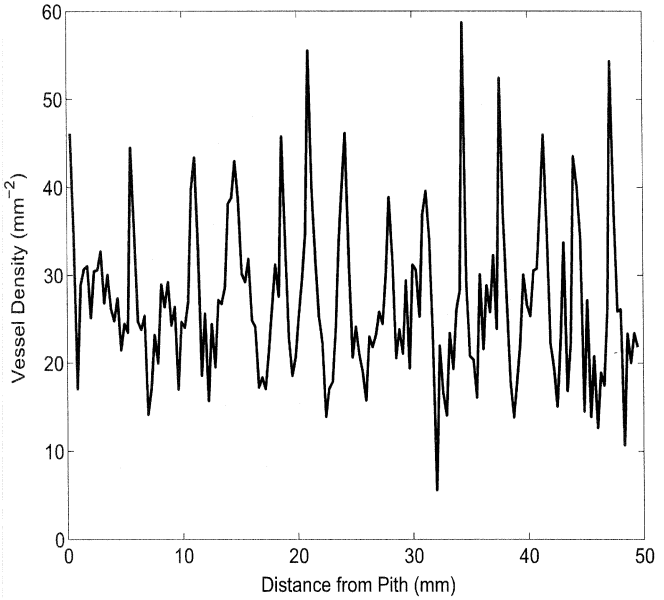

Fig. 6. The vessel density, measured along a transect from pith to bark on a mangrove stem disc, as function of the distance from the pith.

To conclude, the polynomial model of the TBD seems to be better than the trigonometric one to expand to the TBD. In the polynomial model, no systematic errors are present and no arrangements against ringing are necessary. When the trigonometric model is used, without any arrangements, a significant misfit is found due to ringing. The samples near the borders are discarded, which reduces the residual cost function by a factor 30, but 10% of the measurements are lost. The alternative is to enlarge the borders, while the model is still matched on the original time window. The latter has a slightly better performance: no samples are lost, the cost function is reduced by a factor 400, but the bandwidth of the TBD model decreases proportionally to the enlargement.

B. Optimal Size of the Extra Borders

If more lines are added at the borders, the ringing will become smaller. On the other hand, the bandwidth of the TBD model will decrease and this will cause a larger systematic error. So, what is the optimal number of the extra samples at the borders? A strategy is presented to find a rough estimate of the optimal size [35]. To avoid long calculation time, the residual cost function is calculated for three possible enlargements of the borders. A parabolic function is fitted to these three values and the minimum of this parabolic function is chosen as an optimal value (for example, $p = \{1, 10, 20\}$). This procedure is illustrated on the simulation presented in the previous paragraph and seems to work well as long as the optimal value is between the initial values. Fig. 5 shows the cost function as function of the border size q. The optimal value for this case study is an enlargement of 26%, i.e., $q = 13$ (the number of extra samples at each border). The predicted values are distributed around this value with a mean of 13.6 samples and a standard deviation of 1.7 samples, depending on the chosen values of the enlargement. The actual value depends slightly on the choice of the initial values, but the value of the cost function hardly differs within the interval defined by twice the standard deviation, as can be seen in Fig. 5. A good choice of the enlargement parameter p can reduce the cost function substantially: 60 dB in this simulation. In real examples, the systematic error caused by the limited bandwidth of the TBD model can be more or less important. So, for each case the enlargement parameter q has to be estimated again. When the bandwidth of the TBD model is increased by increasing the parameter b in (3), the optimal value of q has to be reestimated. Estimating both parameters can be done by employing a model selection criterion [37].

VI. Real-World Application

We now apply this procedure to a record of the vessel density measured along a radius from pith to bark of a mangrove tree from Kenya *(R. mucronata)*. Vessel density may be related to environmental parameters such as temperature and/or precipitation[1] (see [9], [10], and [33]), we can therefore expect periodicity in the signal, which is shown in Fig. 6. The data record is 170 samples long and covers approximately 15 years. Its spectrum is shown in Fig. 7, where we have assumed a constant growth rate of 3.3 mm/y. The annual variation can be seen and has been confirmed [36], but one can wonder if the biannual climatic fluctuations present along the Kenyan coast (see methodology) are reflected in this signal. Growth rate variations make an interpretation of the spectrum hard. For instance, one can wonder what the second peak at 1.25 y^{-1} could mean. In order to give a correct interpretation of the spectrum, we have used the TBD methodology.

A signal model consisting of three harmonics A_k with $k \in \{1, 2, 3\}$, with a fundamental frequency of $\omega = 2\pi 15$ y^{-1}, is

[1]The beginning and ending of each season differs from year to year. These variations can be described by time jitter [2], but this is not handled in this paper.

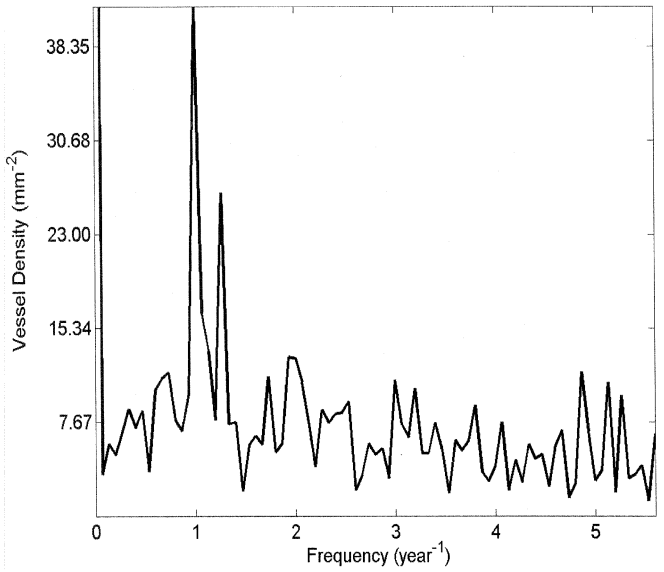

Fig. 7. The spectrum of the vessel density, assuming a constant growth rate.

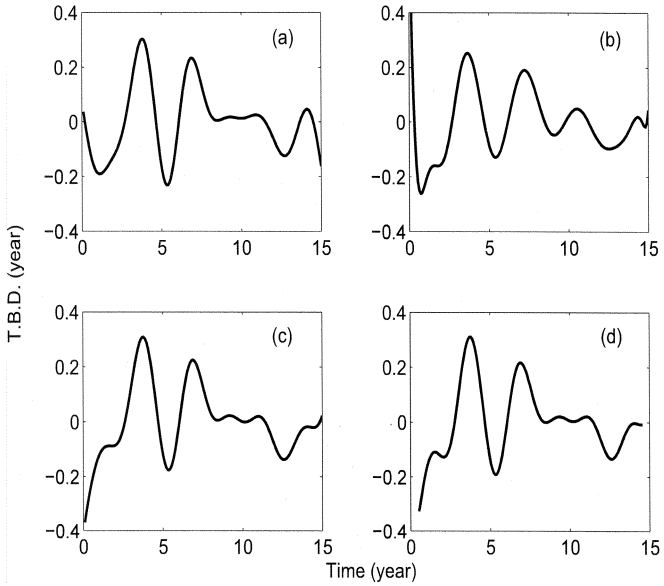

Fig. 8. The different TBDs: (a) Fourier model with ringing, (b) a polynomial model, (c) Fourier model with enlarged borders, and (d) Fourier model with reduced borders.

used; furthermore, the time base model employed 14 parameters B_l with $l \in \{1, \ldots, 14\}$. This model complexity was determined following [37].

The residual cost function obtained from the Fourier model for the TBD on the original data set is 2844 (no removal or addition of samples). The polynomial model with the same number of coefficients gives a slightly better result, 2613. Employing the reduced model, where 5% of the measurements were dropped near each border ($q = 5$), decreases the residual cost functions to 2387 [corrected by (10) for the loss of samples]. The enlarged model, with the optimal value $q = 6$, achieves a similar result: 2343. To conclude, ringing seems responsible for at least 17% of the residual cost function. When ringing is treated, the Fourier model seems to perform better than the polynomial model.

Comparing the different Fourier models (Fig. 8), (a), (c), and (d) show that ringing causes a severe difference in the estimation of the TBD, especially at the borders, e.g., at the left (c) curves down and (a) curves up, whereas the opposite appears at the right side. The general shape of (c) and (d) (Fourier model) compared with (b) (polynomial model) is similar, although local differences are present. Because of a lower cost function, the Fourier models are preferred. Models (c) and (d), both Fourier models without ringing, are very similar, except that (c) also estimates the TBD at the borders.

The objective of the construction of these time bases is the comparison with environmental parameters (see [9] and [33] for more details). In order to illustrate the method, the vessel density signal is compared with the maximum monthly temperature (°C), monthly precipitation (mm), and mean monthly relative humidity (Table I). Environmental data were obtained from the Kenya Meteorological Department in Mombasa. The raw vessel density data were interpolated on the newly reconstructed time frame. When no time base correction was performed, the correlation with environmental parameters was weak. The correlation with the maximum temperature increases from 18% to typically 69% and from minus 28% to typically minus 62% with humidity

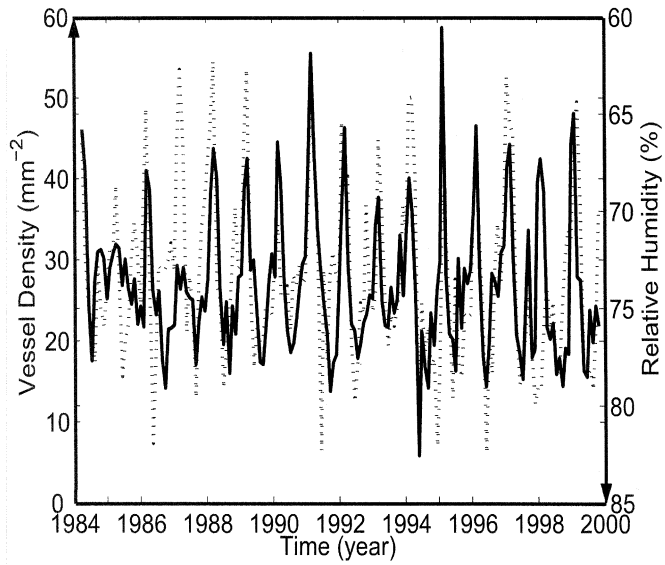

Fig. 9. The vessel density on a corrected time grid (full line) versus the relative humidity (dotted line). To stress the anticorrelation between both, the relative humidity scale was inverted.

when a time base correction is used. Without the time base correction, the misfit is largely due to misfits in the peak's position; with a time base correction, the remaining misfit is mainly due to differences in the amplitude of the peaks (see Figs. 9 and 10). Comparison of the different TBD models in Table I shows that the differences in correlation are too small to distinguish between the different time base distortion models based on the correlation with environmental parameters. When the different environmental parameters are compared with the vessel density, it follows that both temperature and humidity seem to correlate reasonably well with the vessel density. The precipitation signal is much less regular, which is reflected by the weak correlation (see [9] and [33]).

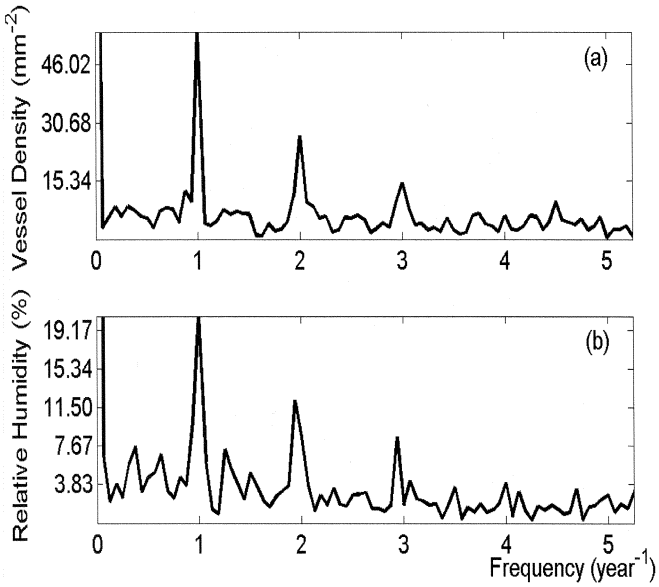

Fig. 10. (a) Spectrum of the vessel density, corrected for variations in growth rate and (b) spectrum of the relative humidity over the last 16 years.

TABLE I
THE CORRELATION COEFFICIENTS CHARACTERIZING THE CORRELATIONS BETWEEN SEVERAL ENVIRONMENTAL PARAMETERS AND THE VESSEL DENSITY, CONSTRUCTED ON DIFFERENT TIME BASES (THE DC COMPONENT WAS REMOVED BEFORE THE CORRELATION COEFFICIENTS WERE CALCULATED)

	Maximum Temperature	Precipitation	Relative Humidity
Constant growth rate	**18%**	**7%**	**-28%**
Polynomial T.B.D. model	**62%**	**10%**	**-56%**
Fourier T.B.D. model with ringing	**66%**	**12%**	**-61%**
Fourier T.B.D. model with reduced borders	**69%**	**9%**	**-61%**
Fourier T.B.D. model with enlarged borders	**69%**	**10%**	**-62%**

VII. CONCLUSION

A time base distortion approach was used to reconstruct time series, e.g., density in a mangrove tree. When a Fourier base was used to model the time base distortion, it was biased due to the Gibbs phenomenon. In order to circumvent this bias, two adaptations were proposed. First, we used a polynomial model for the time base distortion. Under certain circumstances, like slowly varying growth rates, this model outperforms. However, a disadvantage of the polynomial model is that it becomes ill conditioned when the number of basis functions increases. On the contrary, the Fourier series was still well conditioned. Secondly, we have adapted the model based on a Fourier basis by employing a model window that is larger than the measurement window. In these additional borders, ringing occurs. Next, we delete these borders and thus most of the bias. The advantage of enlarging the borders is that no samples are lost. The disadvantage is that the bandwidth of the time base distortion model is smaller. Employing more parameters can remedy this disadvantage.

In the simulation, an exponentially decreasing growth rate was chosen and the Fourier basis with ringing, the polynomial basis, and two Fourier models remedied for ringing were compared. Therefore, we dropped some samples near the borders, as advised in [2], and we enlarged the model window, as described in this paper. Both solutions reduced the ringing considerably, but in this simulation, the polynomial model outperformed. Which basis matches better depends upon the particular growth rate, which is unknown. In our botanical example, the Fourier model, remedied for ringing, matched better, resulting in a lower cost function.

The procedures discussed in this paper are applicable to a wide array of short periodic data records, from both temperate and tropical regions, where all data points are critical. The work of validating and or calibrating environmental proxies often entails correlating short instrumental records (e.g., 2–10 y) with accretionary records (e.g., speleothems, corals, sclerosponges, mollusks) [14], [16], [21], [22], [31], [32]. Such work should greatly benefit from the proposed procedure.

ACKNOWLEDGMENT

The authors would like to thank Dr. I. H. Beeckman (Royal Museum of Central Africa) for his logistical help and D. P. Gillikin for his comments on the manuscript.

REFERENCES

[1] J. Verspecht, "Accurate spectral estimation based on measurements with a distorted-timebase digitizer," *IEEE Trans. Instrum. Meas.*, vol. 43, pp. 210–215, 1994.
[2] J. Schoukens, R. Pintelon, and G. Vandersteen, "A sinewave fitting procedure for characterizing data acquisition channels in the presence of time base distortion and time jitter," *IEEE Trans. Instrum. Meas.*, vol. 46, pp. 1005–1010, 1997.
[3] G. Vandersteen, Y. Rolain, and J. Schoukens, "An identification technique for data acquisition characterization in the presence of nonlinear distortions and time base distortions," *IEEE Trans. Instrum. Meas.*, vol. 50, pp. 1355–1363, 2001.
[4] G. Stenbakken and J. Deyst, "Time-base nonlinearity determination using iterated sine-fit analysis," *IEEE Trans. Instrum. Meas.*, vol. 47, pp. 1056–1061, 1998.
[5] ——, "Comparison of time base nonlinearity measurement techniques," *IEEE Trans. Instrum. Meas.*, vol. 47, pp. 34–39, 1998.
[6] P. Détienne, "Appearance and periodicity of growth rings in some tropical woods," *IAWA Bull.*, vol. 10, no. 2, pp. 123–132, 1989.
[7] P. T. Mushove, J. A. B. Prior, C. Gumbie, and D. F. Cutler, "The effects of different environments on diameter growth increments of *Colophospermum mopane* and *Combretum apiculatum*," *Forest Ecol. Manage.*, vol. 72, pp. 287–292, 1995.
[8] E. C. February and W. D. Stock, "An assessment of the dendrochronological potential of two *Podocarpus* species," *Holocene*, vol. 8, no. 6, pp. 747–750, 1998.
[9] A. Verheyden, "*Rhizophora mucronata* as a proxy for changes in environmental conditions: A study of the wood anatomy, stable isotope chemistry and inorganic composition of a Kenyan mangrove species," Ph.D. dissertation, Vrije Universiteit Brussel, Brussels, Belgium, 2004.
[10] U. Sass and D. Eckstein, "The variability of vessel size in beech (*Fagus sylvatica*) and its ecophysiological interpretation," *Trees—Structure Function*, vol. 9, no. 5, pp. 247–252, 1995.
[11] L. Astrade and Y. Bégin, "Tree-ring response of *populus tremula L.* and *quercus robur L.* to recent spring floods of the Saône River," *Ecoscience*, vol. 4, no. 2, pp. 232–239, 1997.
[12] C. E. Lazareth, P. Willenz, J. Navez, E. Keppens, F. Dehairs, and L. André, "Sclerosponges as a new potential recorder of environmental changes: Lead in *Ceratoporella nicholsoni*," *Geology*, vol. 28, pp. 515–518, 2000.

[13] S. Verheyden, E. Keppens, I. J. Fairchild, F. McDermott, and M. Weis, "Mg, Sr and Sr isotope geochemistry of a Belgian Holocene speleothem: Implications for palaeoclimatic reconstructions," *Chem. Geol.*, vol. 169, pp. 161–144, 2000.
[14] B. E. Rosenheim, P. K. Swart, S. R. Thorrold, P. Willenz, L. Berry, and C. Latkoczy, "High-resolution Sr/Ca records in sclerosponges calibrated to temperature in situ," *Geology*, vol. 32, no. 2, pp. 145–148, 2004.
[15] A. A. Finch, P. A. Shaw, G. P. Weedom, and K. Holmgren, "Trace element variation in speleothem aragonite: Potential for palaeoenvironmental reconstruction," *Earth Planet. Sci. Lett.*, vol. 186, pp. 255–267, 2001.
[16] J. F. Marshall and M. T. McCulloch, "An assessment of the Sr/Ca ratio in shallow water hermatypic corals as a proxy for sea surface temperature," *Geochimica et Cosmochimica Acta*, vol. 66, pp. 3263–3280, 2002.
[17] G. Wei, M. Sun, X. Li, and B. Nie, "Mg/Ca, Sr/Ca and U/Ca ratios of a porities coral from Sanya Bay, Hainan Island, South China Sea and their relationship to sea surface temperature," *Palaeogeog., Palaeoclimatol., Palaeoecol.*, vol. 162, pp. 59–74, 2000.
[18] H. Kuhnert, J. Patzold, B. Schnetger, and G. Wefer, "Sea-surface temperature variability in the 16th century at Bermuda inferred from coral records," *Palaeogeog., Palaeoclimatol., Palaeoecol.*, vol. 179, pp. 159–171, 2002.
[19] S. J. Fallon, M. T. McCulloch, R. van Woesik, and D. J. Sinclair, "Corals at their latitudinal limits: Laser ablation trace element systematics in porites from Shirigai Bay, Japan," *Earth Planet. Sci. Lett.*, vol. 172, pp. 221–238, 1999.
[20] D. J. Sinclair, L. P. J. Kinsley, and M. T. McCulloch, "High resolution analysis of trace elements in corals by laser ablation ICP-MS," *Geochimica et Cosmochimica Acta*, vol. 62, no. 11, pp. 1889–1901, 1998.
[21] C. E. Lazareth, P. E. Vander, L. André, and F. Dehairs, "High-resolution trace element profiles in shells of the mangrove bivalve *Isognomon ephippium*: A record of environmental spatio-temporal variations? Estuarine," *Coastal Shelf Sci.*, vol. 56, pp. 1–12, 2003.
[22] V. E. Putten, F. Dehairs, L. André, and W. Baeyens, "Quantitative in situ microanalysis of minor and trace elements in biogenic calcite using infrared laser ablation—Inductively coupled plasma mass spectrometry: A critical evaluation," *Analytica Chimica Acta*, vol. 378, pp. 261–272, 1999.
[23] G. P. Weedon, "The detection and illustration of regular sedimentary cycles using Walsh power spectra and filtering, with examples from the Lias of Switzerland," *J. Geol. Soc. London*, vol. 146, pp. 133–144, 1989.
[24] T. D. Herbert, "Reading orbital signals distorted by sedimentation: Models and examples," *Spec. Publ. Int. Ass. Sediment*, vol. 19, pp. 483–507, 1994.
[25] D. G. Martinson, N. G. Pisias, J. D. Hays, J. Imbrie, T. C. Moore, and N. J. Shackleton, "Age dating and the orbital theory of the ice age: Development of a high resolution 0 to 300 000-year chronostratigraphy," *Quat. Res.*, vol. 27, pp. 1–29, 1987.
[26] J. Petit, J. Jouzel, D. Raynaud, N. Barkov, I. Basile, M. Bender, J. Chapellaz, J. Davis, G. Delaygue, M. Demotte, V. Kotlyakov, M. Legrand, V. Lipenkov, C. Lorius, L. Pépin, C. Ritz, E. Saltzman, and M. Stievenard, "420 000 years of climate and atmospheric history revealed by the Vostok deep Antarctic ice core," *Nature*, vol. 399, pp. 429–436, 1999.
[27] H. Lieth, J. Berlekamp, S. Fuest, and S. Riediger, "Climate diagrams of the world," in *CD-Series: Climate and Biosphere*, H. Lieth, J. Berlekamp, S. Fuest, and S. Riediger, Eds. Leiden, The Netherlands: Blackhuys, 1999.
[28] R. Pintelon and J. Schoukens, "An improved sine wave fitting procedure for characterizing data acquisition channels," *IEEE Trans. Instrum. Meas.*, vol. 44, pp. 588–593, 1996.
[29] E. V. Putten, F. Dehairs, E. Keppens, and W. Baeyens, "High resolution distribution of trace elements in the calcite shell layer of modern Mytilus edulis: Environmental and biological controls," *Geochimica et Cosmochimica Acta*, vol. 64, pp. 997–1011, 2000.
[30] M. Abramowitz and I. A. Segun, *Handbook of Mathematical Functions with Formulas, Graphs, and Mathematical Tables*. New York: Dover, 1968.
[31] B. Schöne, J. Lega, K. Flessa, D. Goodwin, and D. Dettman, "Reconstructing daily temperatures form growth rates of the intertidal bivalve mollusk *Chione cortezi* (Northern Gulf of California, Mexico)," *Palaeogeog., Palaeoclimatol., Palaeoecol.*, vol. 184, pp. 131–1462, 2002.
[32] D. P. Gillikin, H. Ulens, F. De Ridder, M. Elskens, E. Keppens, W. Baeyens, and F. Dehairs, "Environmental and biological controls on oxygen and carbon isotopes in the aragonitic bivalve *Saxidomus giganteus*: Implications for palaeoclimate studies," Palaeogeog., Palaeoclimatol., Palaeoecol., submitted for publication.
[33] A. Verheyden, F. De Ridder, N. Schmitz, H. Beeckman, and N. Koedam, "Linking vessel density to climate variability in Rhizophora mucronata," Trees—Structure Function, submitted for publication.
[34] R. Pintelon and J. Schoukens, *System Identification: A Frequency Domain Approach*. New York: IEEE Press, 2001.
[35] R. Fletcher, *Practical Methods of Optimization*. Chichester, U.K.: Wiley, 1991.
[36] A. Verheyden, J. G. Kairo, H. Beeckman, and N. Koedam, "Growth rings, growth ring formation and age determination in the mangrove Rhizophora mucronata Lam," *Ann. Botany*, vol. 94, pp. 59–66, 2004.
[37] F. De Ridder, R. Pintelon, J. Schoukens, and D. P. Gillikin, "Modified AIC and MDL model selection criteria for short data records," *IEEE Trans. Instrum. Meas.*, vol. 53, no. 5, pp. 144–150, Oct. 2004.

Fjo De Ridder was born in Leuven, Belgium, on March 30, 1976. He received the Bachelor's degree in chemistry from the Free University of Brussels (VUB), Brussels, Belgium, in 1999, where he is currently pursuing the Ph.D. degree in the Electrical Measurement Department.

He is a Research Assistant. His research is focused on applications of system identification techniques in the field of environmental chemistry (microanalysis of minor and trace elements in biogenic calcite).

Rik Pintelon (M'90–SM'96–F'98) was born in Gent, Belgium, on December 4, 1959. He received the electrical engineering (Burgerlijk Ingenieur) degree, the Doctorate degree of applied sciences, and the qualification to teach at university level (geaggregeerde voor het hoger onderwijs) from Vrije Universiteit Brussel (VUB), Brussels, Belgium, in 1982, 1988, and 1994, respectively.

From October 1982 to September 2000, he was a Researcher with the Fund for Scientific Research–Flanders, VUB. Since October 2000, he has been a Professor in the Electrical Measurement Department, VUB. His main research interests are in the field of parameter estimation/system identification and signal processing.

Johan Schoukens (M'90–SM'92–F'97) was born in Belgium in 1957. He received the engineer degree and the doctoral degree in applied sciences from Vrije Universiteit Brussel (VUB), Brussels, Belgium, in 1980 and 1985, respectively.

He is presently a Professor at VUB. The prime factors of his interest are in the field of system identification for linear and nonlinear systems.

Anouk Verheyden was born in Belgium in 1974. She received the bachelor's degree in biology and the Ph.D. degree in science from Vrije Universiteit Brussel, Brussels, Belgium, in 1997 and 2004, respectively.

While working towards the Ph.D. degree, she studied wood anatomy, stable carbon and isotope chemistry, and inorganic chemistry of mangrove wood. She is currently continuing her research with the Royal Museum for Central Africa, Tervuren, Belgium, where she is involved in a project on tropical dendrochronology.